Journal of Ceramic Processing Research. Vol. 10, No. 1, pp. 85~89 (2009)

J O U R N A L O F
Ceramic Processing Research

High frequency induction heated synthesis and consolidation of nanostructured $ZrSi_2$ from mechanically activated (Zr+2Si) powders

Jeong-Hwan Park[a, b], Kee-Seok Nam[c], Byung-Soo Lee[a], Won-Baek Kim[d] and In-Jin Shon[a,b,*]

[a]*Division of Advanced Materials Engineering, the Research Center of Industrial Technology, Chonbuk National University, 664-14 Deokjin-dong 1-ga, Deokjin-gu, Jeonju, Jeonbuk 561-756, Republic of Korea*

[b]*Department of Hydrogen and Fuel Cells Engineering, Specialized Graduate School, Chonbuk National University, 664-14 Deokjin-dong 1-ga, Deokjin-gu, Jeonju, Jeonbuk 561-756, Republic of Korea*

[c]*Korea Institute of Materials Science 531 Changwondaero, Changwon, Gyeongnam, 641-831, Korea*

[d]*Minerals and Materials Prcessing Division, Korea Institute of Geoscience and Mineral Resources, 30 Gajeong-dong, Yuseong-gu, Daejeon 305-350, Republic of Korea*

Dense nanostructured $ZrSi_2$ was synthesized by a high frequency induction heated combustion synthesis(HFIHCS) method within 3 minutes in one step from mechanically activated powders of Zr and Si. Simultaneous combustion synthesis and consolidation were accomplished under the combined effects of an induced current and mechanical pressure. Highly dense $ZrSi_2$ with a relative density of up to 96% theoretical was produced under simultaneous application of a 60 MPa pressure and the induced current. The average grain size and mechanical properties of the $ZrSi_2$ were investigated.

Key words: High frequency induction heated combustion, Nanostructures; Mechanical properties, $ZrSi_2$.

Introduction

An increase in operating temperature of a gas turbine engine will bring us reductions in both fuel consumption and CO_2 emissions. This requires ultra-high temperature structural materials which overwhelm the performance of nickel-based superalloys commercially used as turbine blade and rotors. Among candidate materials based on refractory metal elements, refractory metal silicides have an attractive combination of properties, including high melting temperature, high modulus, high oxidation resistance in air, and a relatively low density [1, 2]. Furthermore, the disilicides have been used as Schottky barriers, ohmic contacts, gate materials, and interconnectors in intergrated circuits, as a result of their low electrical resistivity, high stability, and good compatibility with silicon substrates [3, 4].

Nanostructured materials have been widely investigated because they display a wide functional diversity and exhibit enhanced or different properties compared with bulk materials [5]. Particularly, in the case of nanostructured ceramics, the presence of a large fraction of grain boundaries can lead to unusual or better mechanical, electrical, optical, sensing, magnetic, and biomedical properties [6-11]. In recent days, nanocrystalline powders have been developed by thethermochemical and thermomechanical processes named the spray conversion process(SCP), co-precipitation and high energy milling [12-14]. However, the grain size in sintered materials becomes much larger than that in the pre-sintered powders due to rapid grain growth during conventional sintering process. Therefore, even though the initial particle size is less than 100 nm, the grain size increases rapidly up to 500 nm or larger during conventional sintering [15]. So, controlling grain growth during sintering is one of the keys to the commercial success of nanostructured materials. In this regard, the high frequency induction heated sintering method which can make dense materials within 2 minutes, has been shown to be effective in achieving this goal [16].

The purpose of this study is to produce dense nanostructured $ZrSi_2$ within 3 minutes in one-step from mixtures of mechanically activated Zr and Si powders using this high frequency induction heated combustion method and to evaluate its mechanical properties (hardness and fracture toughness).

Experimental procedure

Powders of 99.5% zirconium (–325 mesh, Se-jong Products) and 99% pure silicon (–325 mesh, Aldrich Products) were used as a starting materials. Fig. 1 shows the SEM images of the raw materials used. Zr and Si powder mixtures were first milled in a high-energy ball mill, Pulverisette-5 planetary mill at 250 rpm and for 10 h. Tungsten carbide balls (5 mm in diameter)

*Corresponding author:
Tel : +82 63 2381
Fax: +82 63 270 2386
E-mail: ijshon@chonbuk.ac.kr

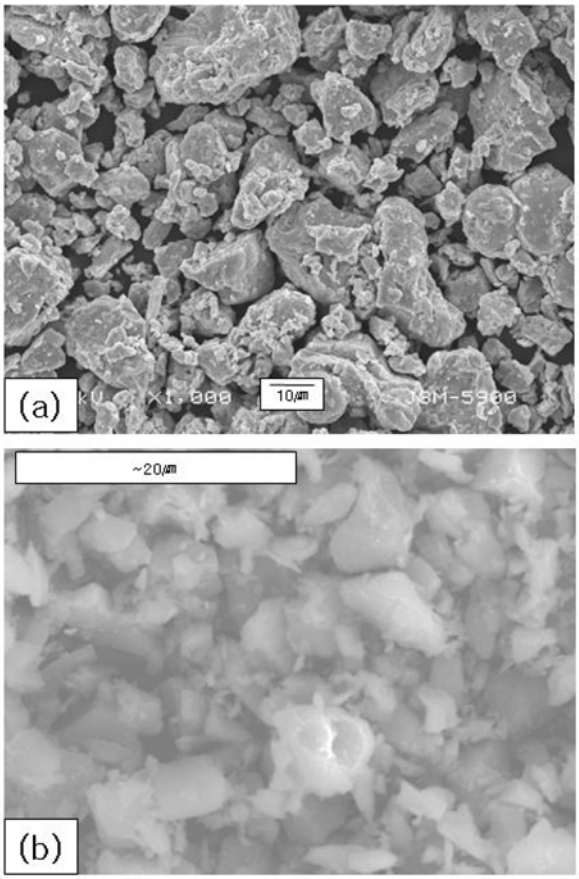

Fig. 1. Scanning electron microscope images of raw materials : (a) Zirconium, (b) Silicon powder.

were used in a sealed cylindrical stainless steel vial under an argon atmosphere. The weight ratio of ball-to-powder was 30:1. Milling resulted in a significant reduction of grain size. The grain size and the internal strain were calculated by Suryanarayana and Grant Norton's formula [17] :

$$B_r\,(B_{crystalline} + B_{strain})\cos\theta = k\lambda / L + \eta\sin\theta \qquad (1)$$

where B_r is the full width at half-maximum (FWHM) of the diffraction peak after instrument correction; $B_{crystalline}$ and B_{strain} are the FWHM caused by the small grain size and internal strain, respectively; k is a constant (with a value of 0.9); λ is the wavelength of the X-ray radiation; L and are grain size and internal strain, respectively; and θ is the Bragg angle. The parameters B and B_r follow Cauchy's form with the relationship: $B = B_r + B_s$, where B and B_s are FWHM of the broadened Bragg peaks and the standard sample's Bragg peaks, respectively. Fig. 2 shows XRD patterns of raw powders and milled Zr + Si powder. The FWHM of the milled powder is wider than that of the raw powder due to an internal strain and a reduction of grain size. The average grain size of Zr measured by Suryanarayana and Grant Norton's equation was about 85 nm.

After milling, the mixed powders were placed in a

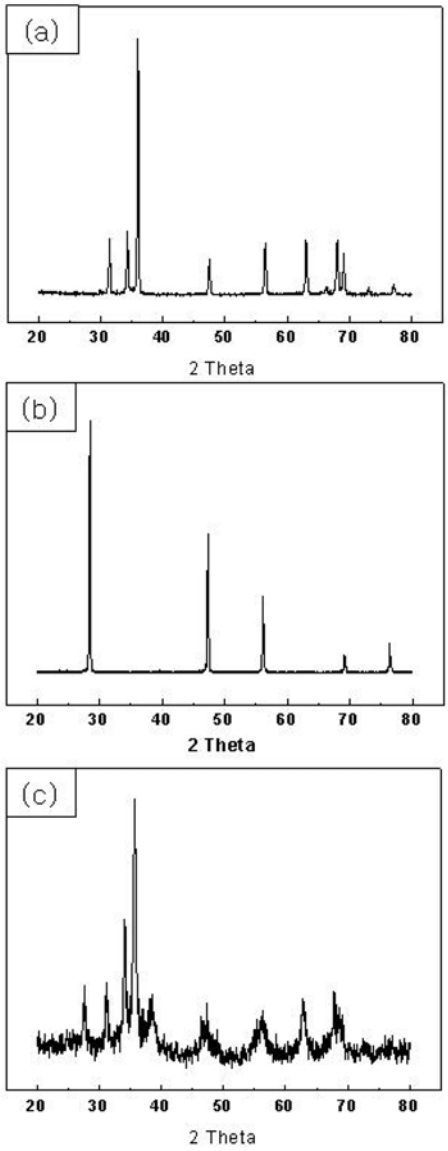

Fig. 2. XRD patterns of raw materials : (a) Zr, (b) Si and (c) milled Zr+Si.

graphite die (outside diameter, 45 mm; inside diameter, 20 mm; height, 40 mm) and then introduced into the induced current activated combustion system made by Eltek in South Korea, shown schematically in Fig. 3. The four major stages in the synthesis were as follows. The system was evacuated (stage 1), and a uniaxial pressure of 60 MPa was applied (stage 2). An induced current (frequency of about 50 kHz) was then activated and maintained until densification was attained as indicated by a linear gauge measuring the shrinkage of the sample (stage 3). Temperature was measured by a pyrometer focused on the surface of the graphite die. At the end of the process, the sample was cooled to room temperature (stage 4). The process was carried out under a vacuum of 40 mtorr (5.33Pa).

The relative densities of the synthesized sample were

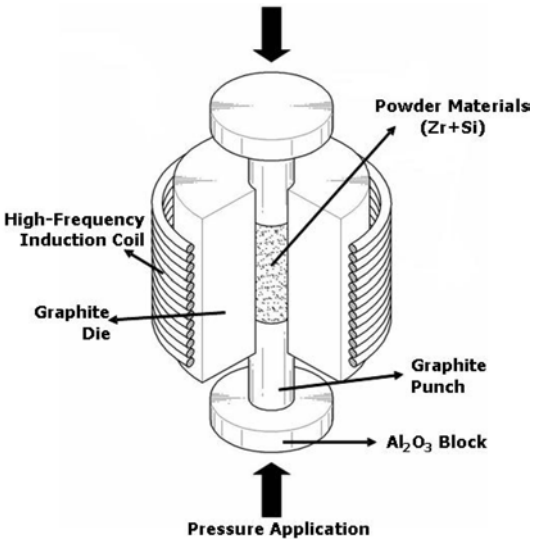

Fig. 3. Schematic diagram of the apparatus for high-frequency induction heated combustion.

measured by the Archimedes method. Microstructural information was obtained from product samples which were polished and etched using a solution of HF (10 vol.%), HNO_3 (20 vol.%) and H_2O (70 vol.%) for 10 s at room temperature. Compositional and micro structural analyses of the products were made through X-ray diffraction (XRD) and scanning electron microscopy (SEM) with energy dispersive X-ray analysis (EDAX). Vickers hardness was measured by performing indentations at a load of 10 kg within a dwell time of 15 s on the synthesized samples.

Results and discussion

The variations in shrinkage displacement and temperature of the surface of the graphite die with heating time during the processing of Zr + Si system are shown Fig. 4 As the induced current was applied the shrinkage displacement initially increased gradually with temperature up to about 550 °C, but then abruptly increased at about 600 °C. Fig. 5 shows the SEM (scanning electron microscope) images of a powder (a) after milling, and a specimen (b) heated to 1,200 °C, respectively. Fig. 5 (a) indicates the presence of the reactants as separate phases. X-ray diffraction results, shown in Fig. 6 (a) exhibit only peaks pertaining to the reactants Zr and Si. However, when the temperature was raised to 1,200 °C, the starting powders reacted producing highly dense products. A SEM image of an etched surface of a sample heated to 1,200 °C under a pressure of 60 MPa is shown in Fig. 5 (b). A complete reaction between these elements (Zr and Si) has taken place under these conditions. These conclusions were supported by X-ray diffraction analyses with peaks of the product phase, $ZrSi_2$ phase, as indicated in Fig. 6 (b). The abrupt increase in the shrinkage displacement at the ignition temperature is due to the increase in density

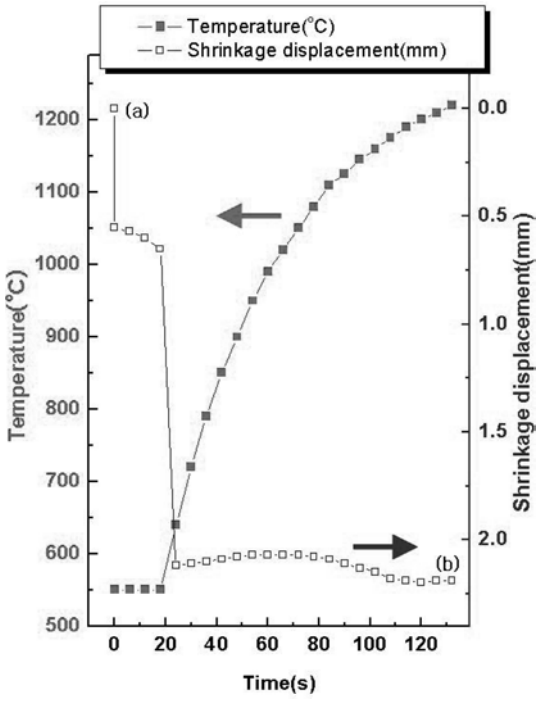

Fig. 4. Variation of temperature and shrinkage displacement with heating time during high-frequency induction heated combustion synthesis and densification of $ZrSi_2$ (under 60MPa, 90% output of total power capacity, 15KW).

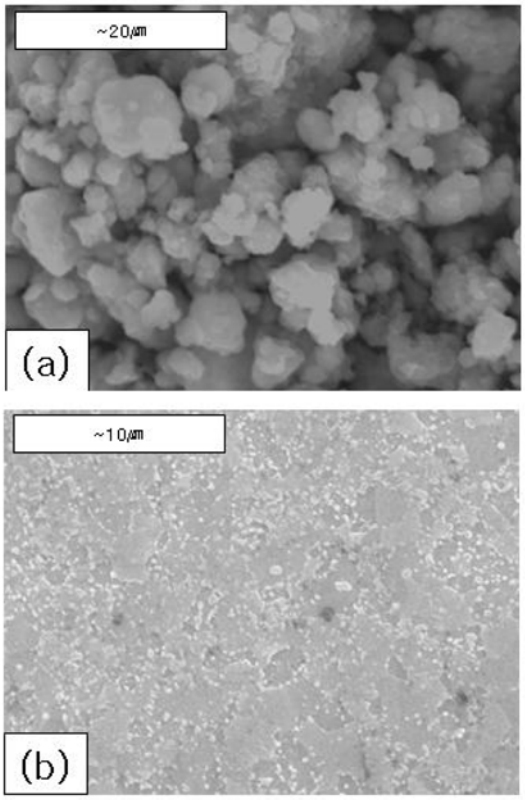

Fig. 5. Scanning electron microscope images of the Zr + Si system : (a) after milling, (b) after combustion synthesis.

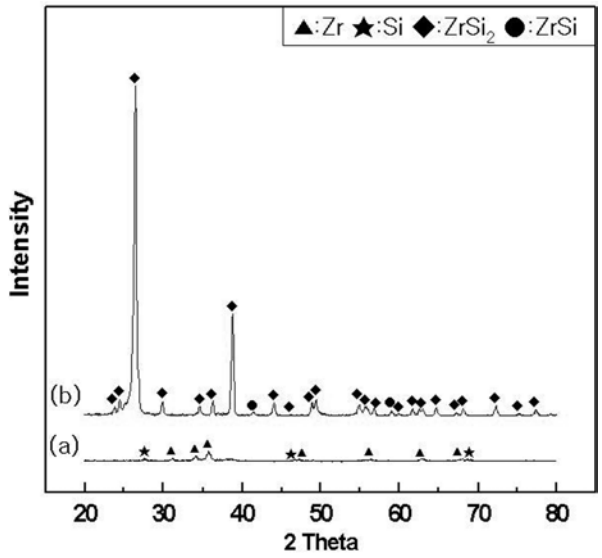

Fig. 6. XRD patterns of the Zr+Si system : (a) after milling, (b) after combustion synthesis.

as a result of the molar volume change associated with the formation of $ZrSi_2$ from Zr+Si reactants and the consolidation of the product. In this study, the ignition temperature of $ZrSi_2$ was below temperature of 600 °C. This temperature is lower than that of the metal silicide reported as about 1,200 °C [18]. It is considered that mechanically activated reactant powders from high energy ball milling can react rapidly to form a compound. The structural parameters, *i.e.* the average grain size of $ZrSi_2$ obtained from Suryanarayana and Grant Norton's formula [17] was 219 nm.

Vickers hardness measurements were made on polished sections of the $ZrSi_2$ using a 10 kg_f load and 15 s dwell time. The calculated hardness value of $ZrSi_2$ was 834 Kg/mm^2. This value represents an average of five measurements. Indentations with large enough loads produced median cracks around the indent. The length of these cracks permits an estimation of the fracture toughness of the materials by means of the expression [19]:

$$K_{IC} = 0.204(c/a)^{-3/2} \cdot H_v \cdot a^{1/2} \quad (3)$$

where c is the trace length of the crack measured from the center of the indentation, a is half of the average length of two indent diagonals, and H_v is the hardness. A typical indentation pattern for a $ZrSi_2$ sample is shown in Fig. 7 (a). Typically, one to three additional cracks were observed to propagate from the indentation corner. The calculated fracture toughness value for the $ZrSi_2$ is approximately 2.3 $MPa \cdot m^{1/2}$. As in the case of the hardness value, the toughness values are an average of five measurements. A higher magnification view of the indentation median crack is shown in Fig. 7 (b). This shows the crack propagates nearly linearly. The absence of reported values for hardness and toughness on $ZrSi_2$ make it difficult to compare to the results obtained in this study to show the influence of grain size.

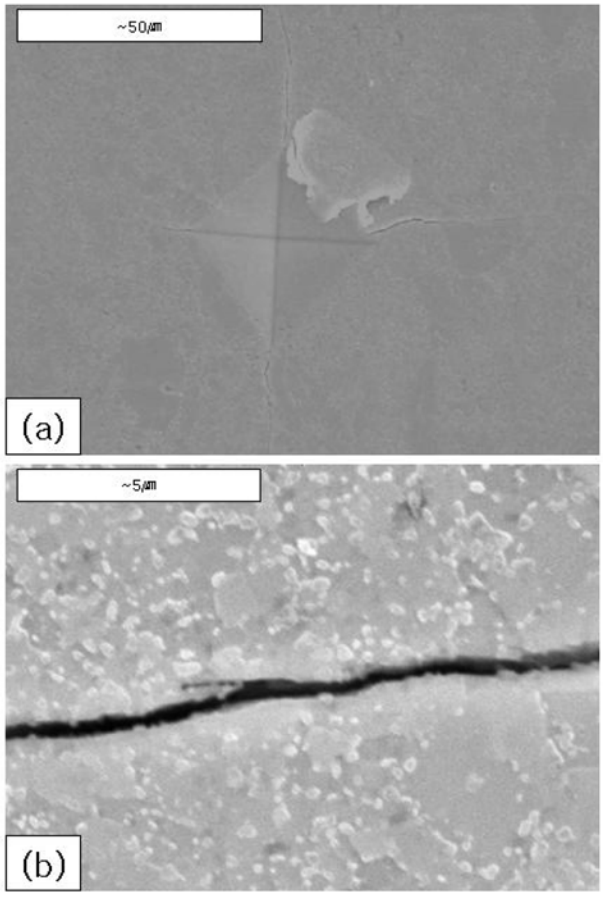

Fig. 7. (a) Vickers hardness indentation and (b) median crack propagating of $ZrSi_2$.

Conclusions

Using the induced current activated combustion method, the simultaneous synthesis and densification of nanostructured $ZrSi_2$ was accomplished from powders of Zr and Si. Complete synthesis and densification can be achieved in one step within duration of 3 minutes. The relative density of the composite was 96% for an applied pressure of 60 MPa and the induced current. The average grain sizes of $ZrSi_2$ prepared by HFIFCS were about 219 nm. The average hardness and fracture toughness values obtained were 834 kg/mm^2 and 2.3 $MPa \cdot m^{1/2}$, respectively.

Acknowledgement

This work was supported by small and midium business administration.

References

1. J.J. Petrovic, A.K. Bhattacharya, R.E. Honnell, T.E. Mitchell, R.K. Wade, and K.J. McClellan, Mater. Sci. Eng. A 155[1-2] (1992) 259-266.
2. GJ. Fan, M.X. Quan, Z.Q. Hu, J. Eckert, and L. Schulz, Scripta Mater. 41[11] (1999) 1147-1151.

3. M.E. Schlesinger, Chem Rev 90(1990) 607-628.
4. A.K. Vasudevan, and J.J. Petrovic, Mater. Sci. Eng. A155[1-2] (1992) 1-17.
5. H. Gleiter, Mater. 6[1-4] (1995) 3-14.
6. J. Karch, R. Birringer, and H. Gleiter. Nature 330 (1987) 556-558.
7. A. M. George, J. Iniguez, and L. Bellaiche, Nature 413 (2001) 54-57.
8. D. Hreniak, and W. Strek, J. Alloys. compd. 341[1-2] (2002) 183-186.
9. C. Xu, J. Tamaki, N. Miura, and N. Yamazoe, Sens. Actuators B 3[2] (1991) 147-155.
10. D.G. Lamas, A. Caneiro, D. Niebieskikwiat, R.D. Sanchez. D. Garcia, and B. Alascio, J. Magn. Mater. 241[2-3] (2002) 207-213.
11. E.S. Ahn, N.J. Gleason, A. Nakahira, and J.Y. Ying, Nano Lett. 1[3] (2001) 149-153.
12. Z. Fang, and J.W. Eason, Int. J. of Refractory Met. & Hard Mater. 13[5] (1995) 297-303.
13. A.I.Y. Tok, L.H. Luo, and F.Y.C. Boey, Mater. Sci. Eng. A 383[2] (2004) 229-234.
14. I.J. Shon, D.K. Kim, I.Y. Ko, J.K. Yoon, and K. T. Hong, Mater. Sci. For. 534-536 (2007) 525-528.
15. M. Sommer, W.D. Schubert, E. Zobetz, and P. Warbichler, Int. J. of Refractory Met. & Hard Mater. 20[1] (2002) 41-50.
16. I.J. Shon, H.K. Park, H.C. Kim, J.K. Yoon, K.T. Hong and I.Y. Ko, Scrip. Mater. 56[8] (2007) 665-668.
17. C. Suryanarayana, M. Grant Norton, "X-ray Diffraction A Practical Approach" (Plenum Press, 1998) 213
18. D.Y Oh, H.C Kim, J.K Yoon, and I.J. Shon, J. Alloy. Compd. 395[1-2] (2005) 174-180
19. K. Niihara, R. Morena, and D.P.H. Hasselman, J. Mater. Sci. Lett. 1[1] (1982) 13-16.